In vivo assessment of size-selective glomerular sieving in transplanted human induced pluripotent stem cell-derived kidney organoids

Berg, C.W. van den; Koudijs, A.; Ritsma, L.; Rabelink, T.J.

RAPID COMMUNICATION www.jasn.org

In Vivo Assessment of Size-Selective Glomerular Sieving in Transplanted Human Induced Pluripotent Stem Cell–Derived Kidney Organoids

Cathelijne W. van den Berg,[1,2] Angela Koudijs,[1,2] Laila Ritsma,[3] and Ton J. Rabelink[1,2]

[1]Department of Internal Medicine–Nephrology, Leiden University Medical Center, Leiden, The Netherlands
[2]Einthoven Laboratory of Vascular and Regenerative Medicine, Leiden University Medical Center, Leiden, The Netherlands
[3]Department of Cell and Chemical Biology, Cancer Genomics Centre Netherlands, Leiden University Medical Center, Leiden, The Netherlands

ABSTRACT

Background The utility of kidney organoids in regenerative medicine will rely on the functionality of the glomerular and tubular structures in these tissues. Recent studies have demonstrated the vascularization and subsequent maturation of human pluripotent stem cell–derived kidney organoids after renal subcapsular transplantation. This raises the question of whether the glomeruli also become functional upon transplantation.

Methods We transplanted kidney organoids under the renal capsule of the left kidney in immunodeficient mice followed by the implantation of a titanium imaging window on top of the kidney organoid. To assess glomerular function in the transplanted human pluripotent stem cell–derived kidney tissue 1, 2, and 3 weeks after transplantation, we applied high-resolution intravital multiphoton imaging through the imaging window during intravenous infusion of fluorescently labeled low and high molecular mass dextran molecules or albumin.

Results After vascularization, glomerular structures in the organoid displayed dextran and albumin size selectivity across their glomerular filtration barrier. We also observed evidence of proximal tubular dextran reuptake.

Conclusions Our results demonstrate that human pluripotent stem cell–derived glomeruli can develop an appropriate barrier function and discriminate between molecules of varying size. These characteristics together with tubular presence of low molecular mass dextran provide clear evidence of functional filtration. This approach to visualizing glomerular filtration function will be instrumental for translation of organoid technology for clinical applications as well as for disease modeling.

JASN 31: 921–929, 2020. doi: https://doi.org/10.1681/ASN.2019060573

Induced pluripotent stem cell (iPSC)–derived kidney organoids are three-dimensional structures grown *in vitro* that exhibit nephrons consisting of glomerular, proximal, and distal tubular structures.[1] Their generation provides opportunities for studying kidney disease, development, and toxicity but potentially, also clinical use as auxiliary tissue therapy for patients with kidney failure. However, these kidney organoids are not yet applicable in regenerative medicine, and several hurdles need to be overcome. For example, kidney organoids *in vitro* lack a functional vascular network, are still immature, and lack a glomerular filtration barrier. The latter comprises the glomerular endothelium, the glomerular basement membrane, and the podocytes, which through intricate cross-signaling and synthesis of an organotypic glycocalyx layer, maintain a size-selective filtration barrier.[2] It is uncertain to what extent the glomeruli in the kidney organoids have proper functional filtration capacity, and their functionality will be key to any potential clinical translation of this technology.

Earlier studies demonstrated that transplantation of embryonic kidney tissue *in vivo* resulted in vascularization primarily by host-derived endothelial cells that migrate into the graft.[3,4] This inspired us and others to transplant kidney organoids under the renal capsule or subcutaneously to allow for their vascularization.[5–7] These studies observed perfused host- and organoid-derived vasculature as well as vascularized glomerular structures.[8] These glomerular structures showed advanced morphologic maturation as did the tubular

Received June 7, 2019. Accepted February 19, 2020.

L.R. and T.J.R. contributed equally to this work.

Published online ahead of print. Publication date available at www.jasn.org.

Correspondence: Dr. Cathelijne W. van den Berg, Department of Internal Medicine–Nephrology, Leiden University Medical Center, Postal Zone C7-Q, Albinusdreef 2, 2333 ZA Leiden, The Netherlands. Email: c.w.van_den_berg@lumc.nl

structures.[6] Upon transplantation, fenestrated glomerular endothelium, a glomerular basement membrane, and extensive podocyte foot processes were formed, raising the question of whether under these conditions the glomeruli also become functional.

In this study, we applied high-resolution intravital imaging that allowed the visualization and functional assessment of glomerular filtration and glomerular barrier function in the transplanted kidney organoids by live *in vivo* imaging of dextran sieving and albumin retention.

METHODS

Full details are provided in Supplemental Material.

Pluripotent Stem Cell Culture and Organoid Differentiation

Human induced pluripotent stem cells (hiPSCs; reporter hiPSC MAFB:mTagBFP2 [hiPSC-MAFB-BFP (blue fluorescent protein)][9]) were maintained in Essential 8 medium and differentiated using previously described protocols.[6,10] Briefly, hiPSCs were incubated for 4 days in 8 μM CHIR99021 in STEMdiff APEL2 medium. On day 4, growth factors were changed to 200 ng ml^{-1} rhFGF9 and 1 μg ml^{-1} heparin. On day 7, cells were transferred as small clumps to three-dimensional culture on Transwell 0.4-μm pore polyester membranes and maintained for another 18 days.

Animal Experiments and Intravital Microscopy

All animal experimental protocols were approved by the animal welfare committee of the Leiden University Medical Center and the Dutch Animal Experiments Committee. Kidney organoids (day 25; cultured 7 days in monolayer and 18 days as a three-dimensional structure) were transplanted under the renal capsule of the left kidney in non-obese diabetic/severe combined immunodeficiency (NOD/SCID) 8 week old mice.[6] A titanium imaging window was implanted on top of the kidney organoid.[6,11,12] One, 2, and 3 weeks after surgery, the mice were intravitally imaged on a Zeiss LSM 710 NLO upright multiphoton microscope equipped with a Mai Tai Deep See multiphoton laser (690–1040 nm) (Supplemental Table 1). *Via* a tail vein cannula, mice were injected with low molecular mass 10, 20, or 40 kDa (rhodamine B isothiocyanate [RITC] or tetramethylrhodamine [TRITC]) dextran; high molecular mass 70, 500, or 2000 kDa dextran (fluorescein isothiocyanate [FITC]), or bovine-albumin (FITC) during image recording (Supplemental Table 2). Glomeruli were recorded (Zeiss Zen software) with time-lapse series containing 3000 images; mice were injected at 50 images (24 seconds). Series were collected in 12 bit and 512×512 pixels, with a resolution of 0.48 seconds at a single Z plane for time series or 1–1.5 μm for Z stacks and tile scans. Fluorophores were excited at 800 nm, and emission was collected in three NDDs: mTagBFP2 (460–500 nm), FITC (510–550 nm), and TRITC (575–620 nm).

Analyses and Calculation

Analyses of intravital microscopy time series were performed with ImageJ Fiji, Microsoft excel spreadsheets, and Graphpad Prism. Three-dimensional reconstructions were made using Imaris and Maxon Cinema4D. Regions of interest in the blood vessel, Bowman's capsule, and extracellular space were defined manually (Supplemental Figure 1). Fluorescence intensity was measured, background fluorescence (average of the first 50 images in time series before dextran infusion) was subtracted, and values were normalized to the highest fluorescence intensity in the blood vessel area and plotted over time. The glomerular sieving coefficient was calculated as the ratio between the fluorescence intensity in specified region of interest: Bowman's space and blood vessel for low molecular mass and high molecular mass dextran molecules.[13] Time point 0 was defined as the highest fluorescence intensity for low molecular mass dextran in the Bowman's capsule. Erythrocytes (visible as dark streaks in the blood vessel) were eliminated from the analysis using the threshold function in ImageJ Fiji.[13,14] Line scans of approximately 135 μm were obtained for several time points on dextran infusion and normalized to the highest intensity in the blood vessel area at the time point immediately after injection of 10 kDa dextran (3.39 minutes). Line scans were plotted for Bowman's capsule, extracellular space, and blood vessels.

Significance Statement

The ability to differentiate human induced pluripotent stem cells to kidney organoids *in vitro* holds promise for disease modeling, drug discovery, and clinical application. The authors differentiated such cells to kidney tissue comprising glomerular, proximal, and distal tubular structures. Earlier research demonstrated that these structures become vascularized upon transplantation in mice and show advanced maturation. To investigate whether human induced pluripotent stem cell–derived kidney organoids can also become functional *in vivo*, they applied high-resolution intravital multiphoton imaging through a titanium imaging window. They demonstrated *in vivo* glomerular filtration and size-selective glomerular barrier function in the transplanted organoids. This technique can be instrumental for further developing stem cell–derived organoids toward clinical applications.

Immunofluorescence Analyses

Organoids under the renal capsule of mouse kidneys were fixed in 4% paraformaldehyde overnight (pH 7.4) and further incubated in 30% sucrose in PBS for 8 hours. Tissues were embedded in OCT, frozen using dry ice, and stored at −80°C. The mouse kidneys with the transplanted organoids were sectioned at the cryotome at 5–10 μm. Structures were analyzed for 10 kDa dextran (lysine fixable TRITC) and for lotus tetragonolobus lectin^{+} (LTL^{+}) proximal tubules. Tissues were examined using the White Light Laser Confocal Microscope TCS SP8 using LAS-X Image software (Leica) and Imaris software.

RESULTS AND DISCUSSION

Although several studies have now characterized stem cell–derived kidney organoids at molecular and morphologic levels, functional data are still lacking. One of the basic functions of the kidney is its ability to produce ultrafiltrate in the

glomerulus. The glomerular filtration process is defined as an integrated functional unit where crosstalk between vascular endothelium and podocytes determines the actual filtration process.[2] The defining feature of an ultrafiltration membrane, such as in the glomerulus, is that it can sieve macromolecules on the basis of molecular size. Dextrans are in this respect useful probes of glomerular function. Because dextrans are thought to be neither secreted nor reabsorbed by the renal tubule (except when very small), their plasma and urine concentrations directly reflect glomerular filtration.[15] To this end, we performed live imaging of dextran sieving in hiPSC-derived glomerular structures in 25-day-old kidney organoids using an mTagBFP2 podocyte reporter (MAFB) iPSC line.[9] These organoids were transplanted under the renal capsule in immunodeficient mice followed by the implantation of an imaging window (Figure 1A).

To validate our model and the subsequent observations on glomerular filtration in the transplanted organoid, we first evaluated dextran sieving characteristics of the mouse kidneys on which the organoids were transplanted. Time-lapse images were taken upon intravenous infusion of low molecular mass dextran (10, 20, and 40 kDa; TRITC) and high molecular mass dextran (70 and 500 kDa; FITC). Low molecular mass dextrans appeared rapidly after injection in the tubular structures of the mouse kidney, reaching their peak within 10 minutes followed by an elimination curve (Supplemental Figure 2). The high molecular mass dextrans were retained in the blood and did not appear in the tubular compartment.

We commenced the functional analysis of the glomerular filtration barrier in the organoids by infusing high molecular mass 2000 kDa dextran followed by low molecular mass 10 kDa dextran. This very high molecular mass dextran allows for visualization of the vasculature, whereas the low molecular mass dextran, which is assumed to have a radius of around 2.3 nM, has been shown to filter almost unhindered in the glomerulus.[15] Low molecular mass 10 kDa dextran was sieved into the Bowman's capsule (Supplemental Figure 3) in the organoid glomerulus, reaching a maximum 5 minutes after injection and then, slowly decreasing over time (Figure 1, B–D), probably as reflection of elimination into the tubular compartment of the organoid (see below) as well as simultaneous urinary excretion by the underlying mouse kidney. High molecular mass 2000 kDa dextran was, as expected, exclusively retained in the blood vessels compared with Bowman's capsule or extracellular space (Figure 1, B–D). To directly compare the amount of dextran in the various compartments, we made line scans crossing the blood vessel, the Bowman's capsule, and the extracellular space displaying fluorescence pixel intensities (Figure 1E, Supplemental Figure 4). The low molecular mass 10 kDa dextran was present in all compartments, being highest in the Bowman's space followed by the blood vessel, whereas the presence of the low molecular mass dextran remained very low in the extracellular space. The latter indicates a selectively high permeability of the glomerular capillary bed for the low molecular mass dextrans compared with the other blood vessels in the organoids.

Next, live imaging of the kidney organoids was performed at 1, 2, and 3 weeks after transplantation. We infused different sizes of dextrans simultaneously and recorded a wide-field tile scan (*Z* stack). This unbiased view shows that all glomerular structures were vascularized, and parts of them were sieving the low molecular mass 10 kDa dextran molecules (Figure 2). We subsequently visualized in detail multiple glomeruli at weeks 1, 2, and 3 after transplantation (Figure 3, A and B, Supplemental Table 1). Regions of interest were selected in multiple glomeruli (Supplemental Figure 1A), and fluorescence intensity normalized for maximal low molecular mass or high molecular mass dextran in the blood vessels was measured as a marker of glomerular molecular sieving. Glomerular sieving of low molecular mass 10 kDa dextrans could be observed as soon as 1 week after transplantation, and its sieving characteristics did not change thereafter (Figure 3C, Supplemental Movies 1 and 2). We visualized this in 20 individual glomerular structures in multiple mice that were recorded for approximately 25 minutes at 1, 2, and 3 weeks after transplantation ($n=20$) (Supplemental Tables 1 and 2). These results are in agreement with our earlier study, where we performed large-scale ultrastructural analysis of the transplanted organoids and could demonstrate that hallmarks of glomerular maturation, such as the presence of fenestrated endothelium, a GBM, and podocytes with foot processes, were present as soon as 7 days after transplantation.[6] To exclude that the loss of fluorescence intensity of the low molecular mass dextran in Bowman's capsule was a result of photobleaching caused by continuous imaging, we calculated the fluorescence intensity in glomerular structures that were imaged in tile scans and were located in the overlap region of two different tiles. These specific glomerular structures were imaged twice, with a time delay of a couple of minutes during which the structures were not imaged. Here, without continuous imaging, we also observed a significant decrease in fluorescence intensity of the low molecular mass dextran, demonstrating that this reduction was not due to photobleaching (Supplemental Figure 5).

Although all glomeruli in the organoids were found to be vascularized (or perhaps, nonvascularized glomeruli had regressed), we estimated the number of sieving glomeruli in multiple tile scans and manually recorded movies, and we observed that the number of functional glomerular structures had a median of 40% but was variable between organoids (Figure 3D). Furthermore, filtration dynamics were shown to vary from one glomerulus to another at the same time after transplantation (Figure 3E) as well as the same glomerulus at 2 consecutive weeks in the same organoid (Supplemental Figure 6). This was particularly true for the peak intensities in Bowman's capsule after injection. From our data, we cannot fully explain this, but this could be related to variability in stages of glomerular maturation and

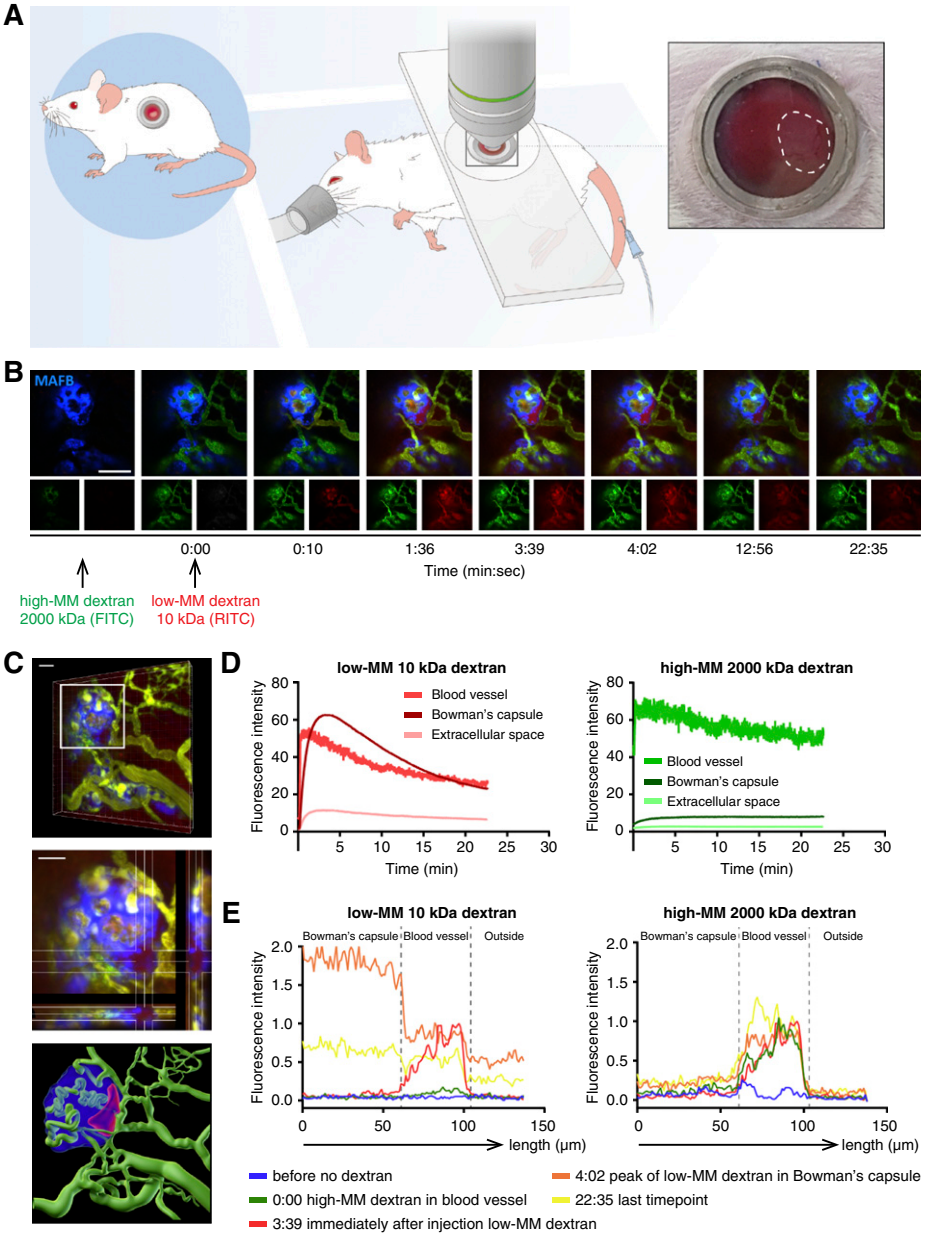

Figure 1. *In vivo* imaging reveals glomerular filtration in transplanted hiPSC-derived kidney organoids. (A) Schematic of experimental setup for intravital imaging of the mouse kidney and transplanted kidney organoids visualized through an implanted imaging window. Dashed line indicates the location of the kidney organoid. (B) Kidney organoids from hiPSC-MAFB-BFP were transplanted and visualized through the imaging window. Still frames from a time series at a single *Z* plane are displayed: merged (upper panels), low molecular mass 10 kDa dextran (FITC; lower left panels), and high molecular mass 2000 kDa dextran (RITC; lower right panels; $n=4$). On infusion, high molecular mass 2000 kDa dextran became apparent in the blood vessels, and low molecular mass 10 kDa dextran was infused at timepoint 0. Low molecular mass 10 kDa dextran initially appeared in the blood vessels only as indicated by the yellow-colored overlay. After 1:36 minutes, low molecular mass 10 kDa dextran fluorescence intensity became visible in the putative Bowman's capsule identified by MAFB-BFP^{+} podocytes in the organoid. At 4.02 minutes, the fluorescence intensity reached its maximum and then, decreased until 22:35 minutes. (C) Three-dimensional view from the *Z* stack of the filtrating glomerular structure (top panel) and orthogonal view of the glomerular structure with its Bowman's capsule in red (middle panel). The bottom panel shows the three-dimensional reconstruction model of vasculature and glomerular structure. (D) Fluorescence intensity low molecular mass 10 kDa dextran (left panel) or high molecular mass 2000 kDa dextran (right panel) in regions of interest (indicated in Supplemental Figure 1A) plotted over time. (E) A line (indicated in Supplemental Figure 1A) (approximately 135 μm) was drawn across the Bowman's capsule, blood vessel, and extracellular space (outside) in still frames from a time series obtained by *in vivo* imaging of the transplanted kidney organoids. Line profiles of the pixel intensities of low molecular mass 10 kDa dextran (left panel) and high molecular mass 2000 kDa dextran (right panel) were obtained for several time points and normalized to the highest intensity in the blood vessel area (3.39 minutes). MM, molecular mass. Scale bars, 100 μm.

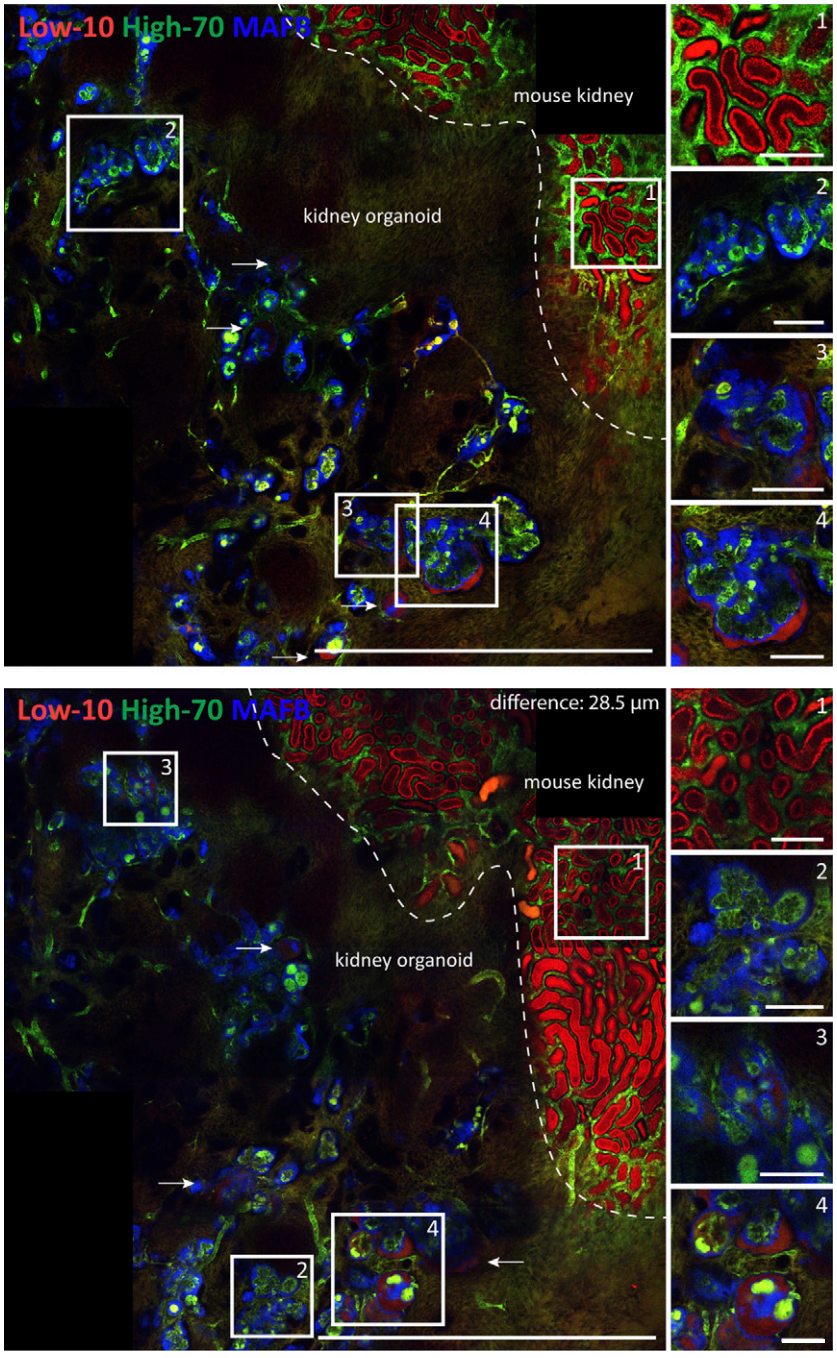

Figure 2. Wide-field evaluation of transplanted organoid through imaging window reveals vascularization of all glomerular structures and sieving of low molecular mass dextran molecules in part of them. (A and B) Tile scan and *Z* stack of a part of the transplanted kidney organoid on top of the mouse kidney at 1 week after transplantation. (1) The mouse kidney can be visualized at the top right corner by reuptake of low molecular mass 10 kDa dextran (TRITC) surrounded by blood vessels (high molecular mass 70 kDa dextran; FITC). The border of the organoid and mouse kidney is indicated by the dashed line. (2) All glomeruli are vascularized, whereas (3 and 4) only a part of them is filtrating. In (B), the same area is displayed 28.5 μm deeper inside the organoid and closer to the mouse kidney. Arrows indicate low molecular mass dextran in Bowman's capsule. Scale bar: 1 mm in left panels; 100 μm in 1–4.

differences between organoid batches[16] as well as pressure-related variation in the vascular beds of the organoids.

To further characterize the size selectivity of the glomerular filtration barrier, we infused different combinations of low molecular mass and larger-sized dextrans as well as albumin to determine the cutoff for size selectivity of the glomerular barrier function. The data show that 70 kDa dextran and albumin (approximately 66 kDa) were retained in the blood vessel and did not appear in the Bowman's space ($n=14$); 20 kDa ($n=6$) and 40 kDa ($n=4$) dextrans were being filtrated into Bowman's space (also on a second infusion), albeit slower than 10 kDa dextran (Figure 4, A–D, Supplemental Figure 7). Also, when 20 and 40 kDa dextrans were serially infused after low molecular mass 10 kDa dextran within 30 minutes, we observed the same filtration curves (Supplemental Figure 8). Together, these data suggest that the glomerular filtration unit is size restricted above 40 kDa ($\pm$4.5 nM). This is also reflected in the calculated glomerular sieving coefficient, which shows an inflection point at this size (Figure 4E). Interestingly, this size restriction of glomerular molecular sieving in the glomerulus of the organoid corresponds well with observations in experimental animals and humans.[15]

To investigate the connection of the glomerular filtration unit to the tubular compartment, we hypothesized that low molecular mass dextran in the filtrate should also be visible in the tubular structures of the organoids. In agreement, tubular presence of low molecular mass 10 kDa molecules was observed intravitally (Figure 4F, Supplemental Figure 9). We also performed additional analyses in fixed tissue sections that demonstrated that low molecular mass 10 kDa dextran was visible in part of the LTL^+ proximal tubular structures, mainly at the apical side of the cells (Figure 4G). This suggests some reuptake and endocytosis of these small dextran molecules in the proximal tubules, thus further corroborating the presence of an active filtration unit.[17,18]

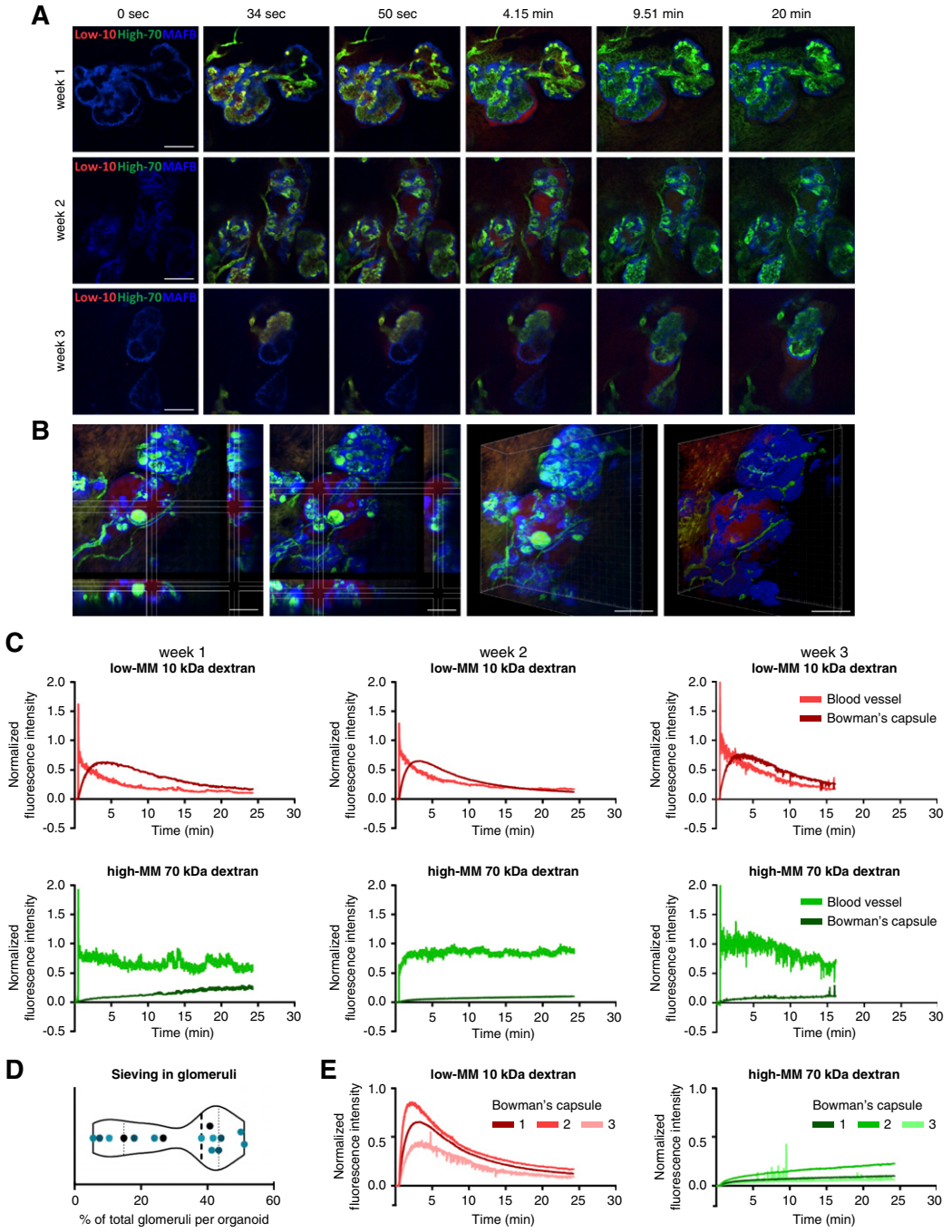

Figure 3. *In vivo* imaging reveals glomerular filtration of low molecular mass 10 kDa dextran and not high molecular mass 70 kDa dextran in transplanted hiPSC-derived kidney organoids. (A) MAFB-BFP^{+} glomeruli were visualized through the imaging window. Low molecular mass 10 kDa dextran (TRITC) and high molecular mass 70 kDa dextran (FITC) were coinjected at 1, 2, and 3 weeks after transplantation in different mice. Sieving of low molecular mass 10 kDa dextran was observed in $n=6$ (week 1), $n=7$ (week 2), and $n=7$ (week 3) mice. Merged still frames from a time series at a single *Z* plane are displayed. (B) Orthogonal view of the glomerular structure with its Bowman's capsule and three-dimensional view from the *Z* stack of the filtrating glomerular structure (Supplemental Movie 2). (C) Normalized fluorescence intensity of low molecular mass 10 kDa dextran (upper panels) and high molecular mass 70 kDa dextran (lower panels) in filtrating MAFB-BFP^{+} structures plotted across time. Regions of interest (other glomerular structures than in [A]) are indicated in Supplemental Figure 1A. Supplemental Movies 1 and 2 display week 2. (D) The number of sieving glomeruli was estimated in multiple tile scans and manually recorded movies as a percentage of the total number of glomeruli per organoid. Each dot represents the percentage of functional glomerular structures that was scored in an individual organoid. (E) Normalized fluorescence intensity plots demonstrate different filtration characteristics in three glomerular structures in three different mice at 2 weeks of transplantation. Regions of interest are indicated in Supplemental Figure 1A. MM, molecular mass. Scale bars, 100 μm.

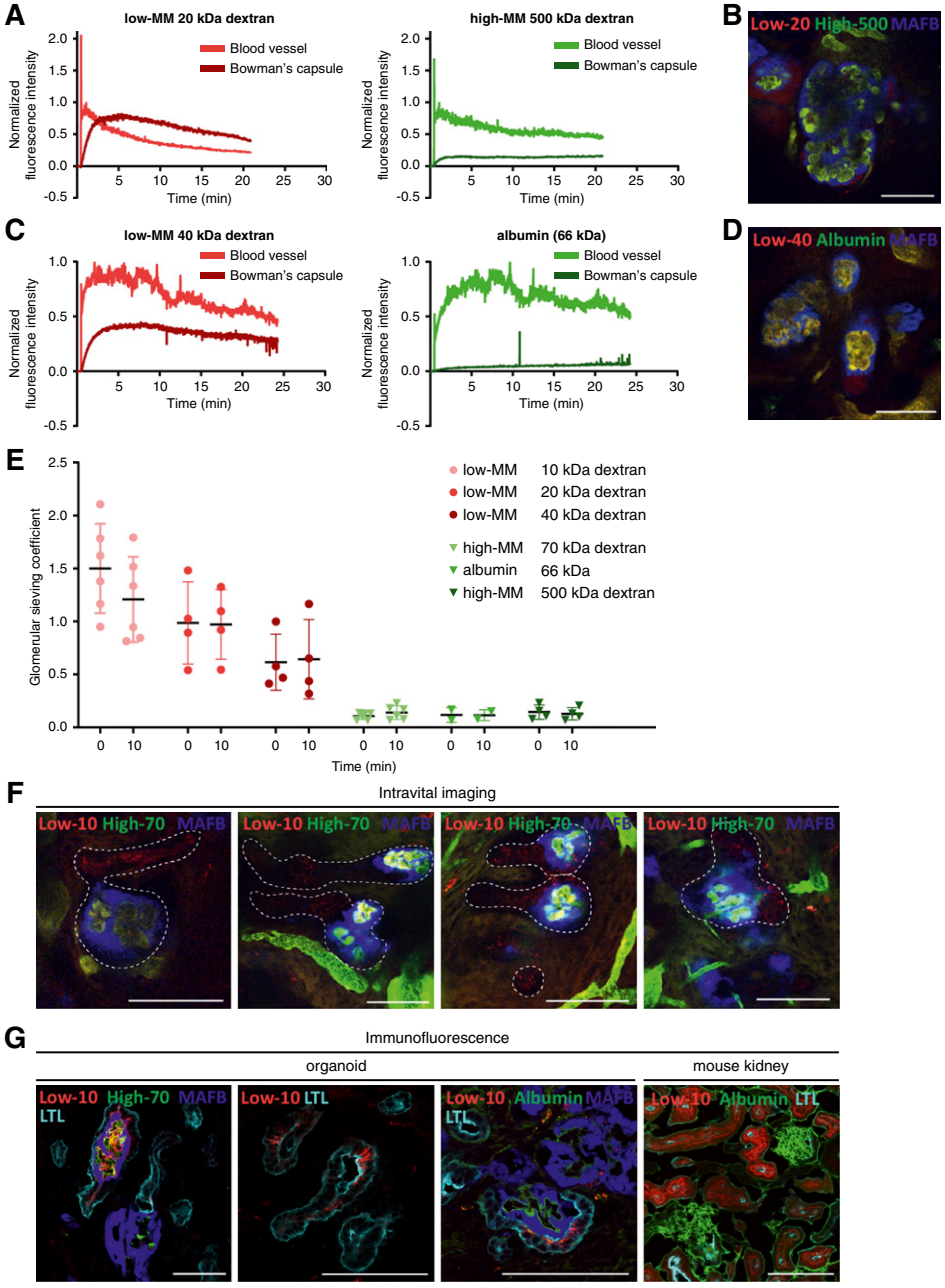

Figure 4. Multiple low and high molecular mass dextran molecules were selectively sieved by the glomeruli and retained in the blood vessels. (A and B) Low molecular mass 20 kDa dextran (TRITC; $n=6$) and high molecular mass 500 kDa (FITC) dextran were infused simultaneously and visualized in MAFB-BFP$^+$ glomerular structures. Normalized fluorescence intensity was plotted across time. Regions of interest are indicated in Supplemental Figure 1A. (C and D) Low molecular mass 40 kDa dextran (TRITC; $n=4$) and albumin (FITC) were infused simultaneously and visualized in MAFB-BFP$^+$ glomerular structures. Albumin is retained in the blood vessels, whereas 40 kDa dextran is filtrated as visualized by the normalized fluorescence intensity across time. Regions of interest are indicated in Supplemental Figure 1A. (E) Glomerular sieving coefficient was calculated from 12 different recordings in nine individual glomerular structures (combined weeks 1, 2, and 3) from five different organoid batches. Glomerular sieving coefficient in glomeruli in kidney organoids was calculated after the low molecular mass has peaked in the Bowman's capsule. Plotted are glomerular sieving coefficients for low molecular mass dextran (10, 20, and 40 kDa), high molecular mass dextran (70 and 500 kDa) at time points 0 and 10 minutes. Error bars indicate SEM. (F) Intravital imaging revealed dextran reuptake in tubular structures. Dotted lines indicate the glomerulus and low molecular mass 10 kDa dextran (TRITC) in the tubular structure. (G) Immunofluorescence demonstrating the presence of low molecular mass 10 kDa dextran (TRITC) in LTL$^+$ proximal tubular structures of transplanted human kidney organoids also adjacent to MAFB-BFP$^+$ glomerular structures. Albumin (FITC) is retained in the blood vessels. Mouse kidney was used as positive control (column 4). MM, molecular mass. Scale bar, 100 μm.

This is the first study to our knowledge that used *in vivo* imaging to show functionality of individual glomerular structures derived from transplanted human cells over time. Our approach demonstrated that hiPSC-derived glomeruli have developed an appropriate barrier function on *in situ* maturation and that they discriminate between molecules of varying size, selectively restricting their passage into Bowman's space. Clearly, there is still a lot to be improved in the patterning of the kidney organoids, and typically, these structures lack stromal organization,[19] such as can also be appreciated from the tile scans in Figure 2. However, next to stromal pattering, vascularization will be instructive and conditional to derive advanced iPSC-derived kidney microtissues. For potential future clinical translation of kidney organoid transplantation, functionality of the glomerular filtration barrier and calculation of GFR will be key elements in the development trajectory to unlock further use of hiPSC-derived kidney organoids both for clinical application as well as for disease modeling.

ACKNOWLEDGMENTS

We acknowledge the support of Marije Koning, Loes E. Wiersma, Ellen Lievers, M. Cristina Avramut, Sophie Dólleman, Dieuwke L. Marvin, Manon Zuurmond, Bernard M. van den Berg, and Cees van Kooten (Leiden University Medical Center, Leiden, The Netherlands). We thank the Light and Electron Microscopy Facility (LUMC) for assistance and maintenance of the microscopes. We thank Melissa Little and Sara Howden (Murdoch Children's Research Institute, Melbourne, Australia) for providing the hiPSC line with MAFB:mTagBFP2 reporter.

Dr. Van den Berg designed and performed experiments, analyzed and interpreted data, and wrote the manuscript. Ms. Koudijs performed experiments. Dr. Ritsma performed experiments, analyzed and interpreted data, and revised the manuscript. Dr. Rabelink interpreted data, wrote the manuscript, and was responsible for funding.

DISCLOSURES

None.

FUNDING

Dr. van den Berg is supported by the Wiyadharma fellowship (Bontius stichting-LUMC). Dr. Ritsma is supported by Veni-grant (Netherlands Organisation for Scientific Research) grant 016.176.081, the Leiden University Medical Center (LUMC), and a subsidy from Leids Universiteits Fonds (LUF) grant CWB 7204. The collaboration with Melissa Little (Murdoch Children's Research Institute, Melbourne, Australia) was supported by National Health and Medical Research Council (NHMRC) grant GNT1156440. This work is supported by the partners of Regenerative Medicine Crossing Borders and Health~Holland, Top Sector Life Sciences & Health.

SUPPLEMENTAL MATERIAL

This article contains the following supplemental material online at http://jasn.asnjournals.org/lookup/suppl/doi:10.1681/ASN.2019060573/-/DCSupplemental.

Supplemental Figure 1. Regions of interest in main figures (A) and regions of interest in supplemental figures (B).

Supplemental Figure 2. Filtration in mouse tubular structures.

Supplemental Figure 3. Scanning Electron Microscopy analysis of glomerular structure after 7 days of transplantation.

Supplemental Figure 4. Fluorescence intensity plot profiles from a time series.

Supplemental Figure 5. Calculation of fluorescence intensity to exclude photobleaching.

Supplemental Figure 6. Filtration in the same glomerular structures at 2 consecutive weeks.

Supplemental Figure 7. Selective sieving and retention of low and high molecular mass dextran molecules.

Supplemental Figure 8. Serial infusion of low molecular mass dextran in the same glomerulus.

Supplemental Figure 9. Time-lapse of low molecular mass 10 kDa dextran detection in tubular structure.

Supplemental Material. Detailed experimental procedures.

Supplemental Movie 1. Time series at a single *Z* plane of glomerular filtration.

Supplemental Movie 2. Three-dimensional view of filtrating glomerular structure.

Supplemental Table 1. Size-selective sieving of dextran molecules in analyzed mice.

Supplemental Table 2. Fluorescent-labeled dextran molecules and albumin.

REFERENCES

1. Little MH, Kumar SV, Forbes T: Recapitulating kidney development: Progress and challenges. *Semin Cell Dev Biol* 91: 153–168, 2019
2. Rabelink TJ, de Zeeuw D: The glycocalyx—linking albuminuria with renal and cardiovascular disease. *Nat Rev Nephrol* 11: 667–676, 2015
3. Dekel B, Amariglio N, Kaminski N, Schwartz A, Goshen E, Arditti FD, et al.: Engraftment and differentiation of human metanephroi into functional mature nephrons after transplantation into mice is accompanied by a profile of gene expression similar to normal human kidney development. *J Am Soc Nephrol* 13: 977–990, 2002
4. Hammerman MR: Renal organogenesis from transplanted metanephric primordia. *J Am Soc Nephrol* 15: 1126–1132, 2004
5. Sharmin S, Taguchi A, Kaku Y, Yoshimura Y, Ohmori T, Sakuma T, et al.: Human induced pluripotent stem cell-derived podocytes mature into vascularized glomeruli upon experimental transplantation. *J Am Soc Nephrol* 27: 1778–1791, 2016
6. van den Berg CW, Ritsma L, Avramut MC, Wiersma LE, van den Berg BM, Leuning DG, et al.: Renal subcapsular transplantation of PSC-derived kidney organoids induces neovasculogenesis and significant glomerular and tubular maturation in vivo. *Stem Cell Reports* 10: 751–765, 2018
7. Bantounas I, Ranjzad P, Tengku F, Silajdžić E, Forster D, Asselin MC, et al.: Generation of functioning nephrons by implanting human pluripotent stem cell-derived kidney progenitors. *Stem Cell Reports* 10: 766–779, 2018
8. Koning M, van den Berg CW, Rabelink TJ: Stem cell-derived kidney organoids: Engineering the vasculature [published online ahead of print December 5, 2019]. *Cell Mol Life Sci* doi:10.1007/s00018-019-03401-0
9. Howden SE, Thomson JA, Little MH: Simultaneous reprogramming and gene editing of human fibroblasts. *Nat Protoc* 13: 875–898, 2018
10. Takasato M, Er PX, Chiu HS, Little MH: Generation of kidney organoids from human pluripotent stem cells. *Nat Protoc* 11: 1681–1692, 2016
11. Ritsma L, Steller EJ, Beerling E, Loomans CJ, Zomer A, Gerlach C, et al.: Intravital microscopy through an abdominal imaging window reveals a pre-micrometastasis stage during liver metastasis. *Sci Transl Med* 4: 158ra145, 2012
12. van Gurp L, Loomans CJM, van Krieken PP, Dharmadhikari G, Jansen E, Ringnalda FCAS, et al.: Sequential intravital imaging reveals in vivo dynamics of pancreatic tissue transplanted under the kidney capsule in mice. *Diabetologia* 59: 2387–2392, 2016

13. Sandoval RM, Molitoris BA: Quantifying glomerular permeability of fluorescent macromolecules using 2-photon microscopy in Munich Wistar rats. J Vis Exp 2013. Available at https://www.jove.com/video/50052/quantifying-glomerular-permeability-fluorescent-macromolecules-using. Accessed March 20, 2019
14. Sandoval RM, Molitoris BA: Intravital multiphoton microscopy as a tool for studying renal physiology and pathophysiology. *Methods* 128: 20–32, 2017
15. Haraldsson B, Nyström J, Deen WM: Properties of the glomerular barrier and mechanisms of proteinuria. *Physiol Rev* 88: 451–487, 2008
16. Phipson B, Er PX, Combes AN, Forbes TA, Howden SE, Zappia L, et al.: Evaluation of variability in human kidney organoids. *Nat Methods* 16: 79–87, 2019
17. Sandoval RM, Molitoris BA: Quantifying endocytosis in vivo using intravital two-photon microscopy. *Methods Mol Biol* 440: 389–402, 2008
18. Schuh CD, Polesel M, Platonova E, Haenni D, Gassama A, Tokonami N, et al.: Combined structural and functional imaging of the kidney reveals major axial differences in proximal tubule endocytosis. *J Am Soc Nephrol* 29: 2696–2712, 2018
19. Wu H, Uchimura K, Donnelly EL, Kirita Y, Morris SA, Humphreys BD: Comparative analysis and refinement of human PSC-derived kidney organoid differentiation with single-cell transcriptomics. *Cell Stem Cell* 23: 869–881.e8, 2018